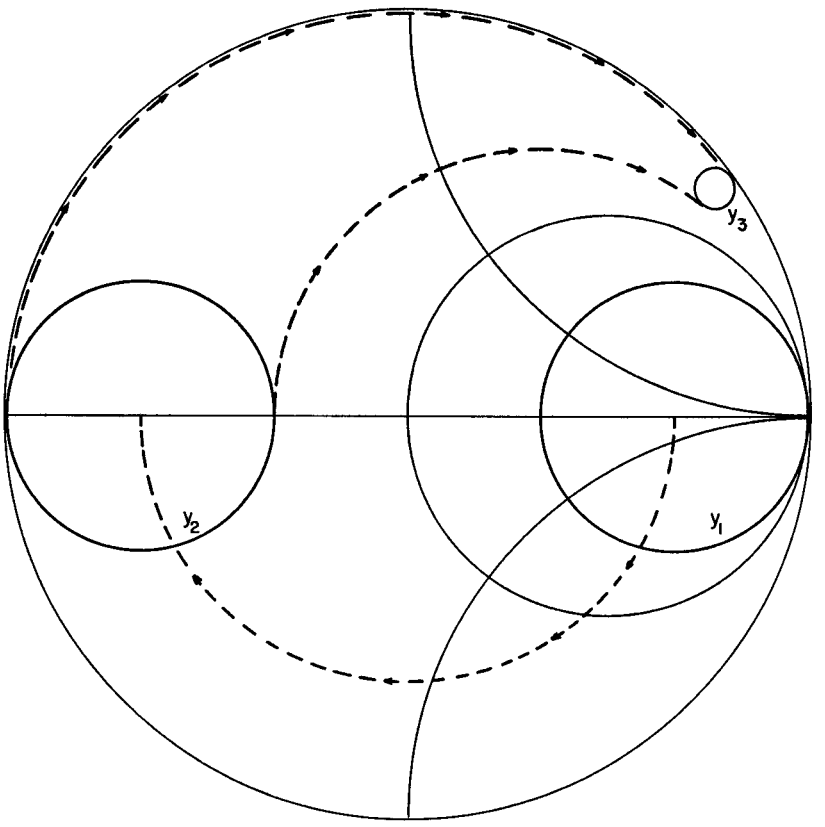

Fig. 2. Modification of Smith-chart admittance diagram by addition of shunt susceptance $j(B/Y_0)=j3.0$ at DS $\pm \frac{1}{4}\lambda_g$.

DS $\pm \frac{1}{8}\lambda_g$, the size of the circle, and hence the coupling coefficient, can be either increased or decreased, depending on the sign of the susceptance being added. The magnitude of the desired susceptance is easily obtained by fitting an admittance circle of the desired size between the appropriate constant-conductance contours, such as the dashed lines connecting y_2 and y_3 in Fig. 2, and observing the difference, in terms of susceptance, between the shifted admittance circle y_2 and the desired admittance circle y_3.

Experimental Results and Conclusion

The experimental cavity consisted of a three-inch section of ring-bar slow-wave structure that was mounted between transverse shorting planes,[4] and that possessed a longitudinal resonance at 1090 MHz. Coupling was achieved by direct connection of the center conductor from a BNC terminal to a ring near one end of the cavity.

In order to modify the coupling to this resonant mode a single stub tuner (modified Weinschel DS 109L) was used to produce $jB/Y_0=j1.0$ at a position $DS+0.89\lambda_g$ "towards load," i.e., the tuner was placed between the cavity and the DS position. Physically, the tuner was located within less than $\frac{1}{2}\lambda_g$ from the cavity terminal. The results are summarized in Table I.

It is seen that by attaching the stub tuner,

TABLE I

Quantity	Without stub tuner	With stub tuner set to give $jB/Y_0=j1.0$
Q_0	111	90
Q_{ext}	53	22
Q_L	36	18
β	2.1	4.1 measured 5.5 predicted

Q_L is decreased by a factor of two. The "predicted" $\beta=5.5$ was obtained by graphically adding the shunt susceptance (assumed constant) to the rotated admittance circle, as was explained. This compared with a measured $\beta=4.1$, with the stub tuner attached. Since both this discrepancy and the change in Q_0 are somewhat greater than might be expected from measurement error, one suspects that in this case the energy stored and dissipated *outside* the cavity was not negligible. In subsequent measurements the setting of the stub tuner was varied to produce a wide range of values for Q_{ext}, but no further significant change was observed in Q_0 ($Q_{ext}=49$, 70, 87, 125 with $Q_0=88$, 86, 87, 92). The apparent change in Q_0 that occurred when the stub tuner was first inserted into the feeder line, was, therefore, probably due to residual reflections from the tuner or its type N connectors, rather than to excessive tuner susceptance as one would at first expect. Clearly, the method does afford a quick and simple way of changing the cavity loading, provided that the shunt susceptance (including residual reflections) is limited to reasonably small values.

[4] B. Kulke, "An extended-interaction klystron: efficiency and bandwidth," Microwave Lab., Stanford University, Stanford, Calif., M.L. Rept. 1320, ch. 4, May 1965.

List of Symbols

β coupling coefficient.
Q_0, Q_{ext}, Q_L internal, external, and loaded Q.
DS detuned-short.
Z_0, Y_0 characteristic impedance, admittance of feeder line.
B shunt susceptance.
l distance between DS and shunt susceptance.
λ_g guide wavelength in feeder line.

Acknowledgment

The author is indebted to Prof. M. Chodorow, of Stanford University, Stanford, Calif., for several stimulating discussions.

Bernhard Kulke
Dept. of Elec. Engrg.
Syracuse University
Syracuse, N. Y.

The Point-Matching Method for Interior and Exterior Two-Dimensional Boundary Value Problems

There have appeared recently some papers [1]–[4] on a "point-matching method" for solving electromagnetic boundary value problems. The only attempts at justifying its use have been qualitative, but the method is plausible, and in some instances gives accurate results. Nevertheless, the method is unsound, in general, as has been pointed out by Harrington [5]. It will be demonstrated, however, that when certain symmetries are maintained, the point-matching method is valid. These symmetries are maintained, or nearly maintained, in the majority of test cases used for "demonstrating" the validity of the method, which explains its apparent success.[1] Yee [6] and Laura [7], [8] describe the background of the method and the motivation for its use.

A single type of electromagnetic boundary value problem will be considered: an infinite, perfectly conducting, cylindrical boundary of arbitrary cross section with the (monochromatic) electric field parallel to the axis of the cylindrical boundary. This type of problem is adequate both for explaining the successes of the point-matching method in special cases and for displaying its inadequacy in general. Figure 1 shows an infinite cylindrical boundary C, supposed perfectly conducting, described by the cylindrical polar coordinates r and θ. The point P at which the field is observed is described by the cylindrical polar coordinates ρ and ϕ. The electric field is constrained to be perpendicular to the paper so that the fields are most conveniently represented by the component of the vector poten-

Manuscript received July 5, 1966; revised October 3, 1966.

[1] It is interesting that these symmetries are maintained in all of the actual calculations quoted by Yee and Audeh [13] in a recent paper.

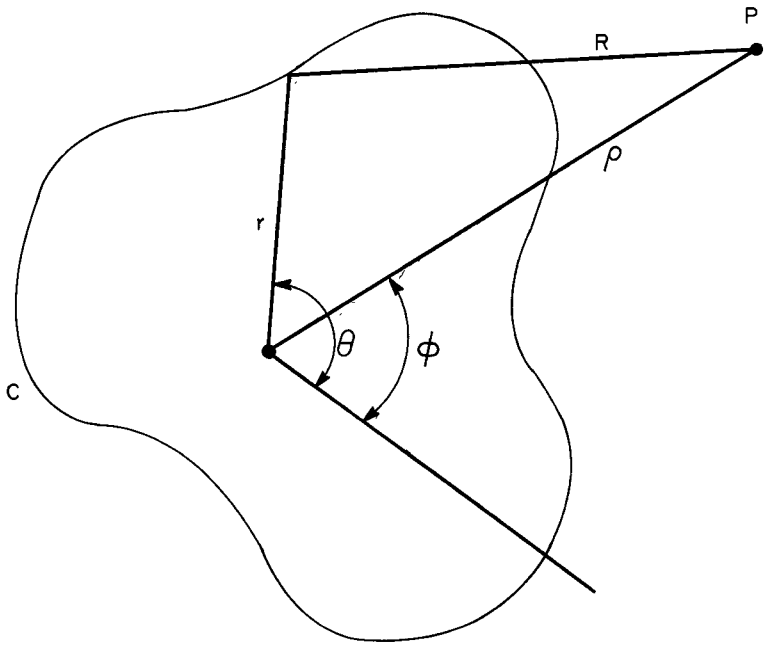

Fig. 1. Geometry for two-dimensional electromagnetic boundary value problem.

tial perpendicular to the paper. Let V be this component of the vector potential. Put

$$V(\rho, \phi) = V_1(\rho, \phi) + V_2(\rho, \phi) \quad (1)$$

where V_1 represents the incident field and V_2 represents the field radiated from C. A convenient and exact form for V_2 is [9] (suppressing the time factor $\exp(j\omega t)$)

$$V_2(\rho, \phi) = \int_C F(C) H_0^{(2)}(kR) dC \quad (2)$$

where F is $-j/4$ times that component (the only component) of the surface current density perpendicular to the paper. Two types of problems will be considered.

a) An interior problem in which there is no incident field and the radiated field is confined to the inside of C. The problem is to find the cutoff wave numbers of E-modes in a waveguide with perimeter C. Thus, since the total field must be zero on C and since the radiated field is the only field,

$$V_1 \equiv 0, \qquad V_2(r, \theta) = 0. \quad (3)$$

In the point-matching method it is assumed that the only important constraint is that the field should be finite everywhere inside C so that V_2 can be meaningfully approximated by

$$V_2(\rho, \phi) = \sum_{m=-M}^{M} A_m J_m(k\rho) \exp(jm\phi) \quad (4)$$

everywhere inside and on C. A solution is obtained by satisfying (3) and (4) at $(2M+1)$ points on C.

b) An exterior problem in which a plane wave, incident at angle ψ, is scattered from C. Thus,

$$V_1(\rho, \phi) = \exp[jk\rho \cos(\phi - \psi)],$$
$$V(r, \theta) = 0. \quad (5)$$

In the point-matching method it is assumed that the only important constraint is the radiation condition at infinity so that V_2 can be meaningfully approximated by

$$V_2(\rho, \phi) = \sum_{m=-M}^{M} B_m H_m^{(2)}(k\rho) \exp(jm\phi) \quad (6)$$

everywhere outside and on C. A solution is obtained by satisfying (5) and (6) at $(2M+1)$ points on C.

The validity of the expressions (4) and (6) will now be examined, the analysis being based upon (2), which is exact. The addition theorem for Bessel functions [10] can be used to expand the Hankel function in (2). Thus, for ρ greater and less than r, respectively,

$$V_2(\rho > r, \phi) = \sum_{m=-\infty}^{\infty} H_m^{(2)}(k\rho) \cdot \exp(jm\phi) \int_C F(C) J_m(kr) \exp(-jm\theta) dC$$

$$V_2(\rho < r, \phi) = \sum_{m=-\infty}^{\infty} J_m(k\rho) \cdot \exp(jm\phi) \int_C F(C) H_m^{(2)}(kr) \cdot \exp(-jm\theta) dC. \quad (7)$$

Take a particular point (r, θ) on C. Denote any other point on C by (s, v). Separate C into the two parts, $\alpha(r)$ and $\beta(r)$, on which s is less than or greater than r, respectively. Thus,

$$\alpha(r) \cup \beta(r) = C, \quad \alpha(r) \cap \beta(r) = 0,$$
$$s \lessgtr r \text{ in } \begin{matrix} \alpha(r) \\ \beta(r) \end{matrix}. \quad (8)$$

From (7) and (8) when the point P is on C, which is to say, when $(\rho, \phi) = (r, \theta)$,

$$V_2(r, \theta) = \sum_{m=-\infty}^{\infty} \left[H_m^{(2)}(kr) \int_{\alpha(r)} F(C) J_m(ks) \cdot \exp(-jmv) dC + J_m(kr) \int_{\beta(r)} F(C) H_m^{(2)}(ks) \cdot \exp(-jmv) dC \right] \exp(jm\theta). \quad (9)$$

Now consider the interior problem posed in a). The conditions (3) have to be satisfied. Manipulating (9) and retaining only the first $(2M+1)$ Fourier coefficients, and using (8), gives

$$\sum_{m=-M}^{M} J_m(kr) \exp(jm\theta) \int_C F(C) J_m(ks) \cdot \exp(-jmv) dC - j \sum_{m=-M}^{M} \left[Y_m(kr) \int_{\alpha(r)} F(C) J_m(ks) \cdot \exp(-jmv) dC + J_m(kr) \int_{\beta(r)} F(C) Y_m(ks) \cdot \exp(-jmv) dC \right] \exp(jm\theta) = 0. \quad (10)$$

It can be seen immediately that the expansion (4), which is used in the point-matching method, is incomplete. To the right-hand side of (4) should be added another summation involving the functions $Y_m(k\rho)$. Furthermore, the coefficients of this second expansion will be functions of ρ, as can be seen from either (7) or (10). Consequently, unless C is nearly circular V_2 cannot be meaningfully approximated in general by the right-hand side of (4) if the coefficients A_m are constants. However, there are particular instances, when C is not nearly circular, when (4) is a meaningful approximation. Suppose that C is a curve symmetric about $\theta = 0$, and also that $F(C)$ is real and even, or pure imaginary and odd. These conditions apply to any symmetric or antisymmetric mode in a waveguide with a cross section exhibiting a plane of symmetry (in fact, any practical waveguide of impeccable manufacture). When these conditions apply $V_2(r, \theta)$, as given by (4), is the real part of the left-hand side of (10). Since the real part must be zero independently of the imaginary part, the point-matching method is valid in this instance, which explains the successes of Yee and Audeh [3], [4]. Now consider the exterior problem posed in b). Conditions (5) have to be satisfied. Expanding V_1 in its Fourier series in ϕ, manipulating (9), using (8), and retaining only the first $(2M+1)$ Fourier coefficient gives

$$\sum_{m=-M}^{M} \left\{ j^m J_m(kr) + H_m^{(2)}(kr) \int_C F(C) J_m(ks) \cdot \exp(-jmv) dC - j \left[J_m(kr) \int_{\beta(r)} Y_m(ks) - Y_m(kr) \int_{\beta(r)} J_m(ks) \right] F(C) \exp(-jmv) dC \right\} \cdot \exp(jm\theta) = 0. \quad (11)$$

Comparison of (6) and (11) shows that the quantity in the inner square bracket in (11) must be negligible if the point-matching method is to be valid. When C is nearly circular, as in the work of Mullin et al. [1], the quantity in the inner square bracket is clearly small (in fact, an estimate of the magnitude of this quantity could be used to estimate the accuracy of the types of calculation carried out by Mullin et al. [1]). The point-matching method would also be valid for problems in which the following conditions were applicable. If C is symmetric about $\theta = 0$ and if $F(C)$ is real and even, then the quantity in the inner square bracket in (11) will cancel if (11) is added to its complex conjugate. Unfortu-

nately, these conditions seem to apply only to a plane wave normally incident upon an infinite flat sheet. Consequently, the point-matching method appears to be a meaningful approximation for nontrivial exterior boundary value problems only if C is nearly circular.

It is certainly easier to write down the equations for the point-matching method than for either the exact integral equation method [11] or the exact extended boundary condition method of Waterman [12], both of which can be based on (2). However, the computational effort required to reach a solution cannot be significantly less for the point-matching method, even though the exact methods involve more work in the setting up of the main computations (a subtle distinction which was pointed out by a reviewer). For equal accuracy (in those instances when the point-matching method is valid) at least as many linear algebraic equations must be solved simultaneously (it is the solution of these equations which absorbs the major part of the computational effort). Consequently, it is suggested that the point-matching method should be discarded in favor of either Harrington's [5] proposed extension of the method or the exact methods [11], [12].

R. H. T. Bates[2]
Dept. of Elec. Engrg.
University of Canterbury
Christchurch, New Zealand

References

[1] C. R. Mullin, R. Sanbury, and C. D. Velline, "A numerical technique for the determination of scattering cross sections of infinite cylinders of arbitrary geometrical cross section," *IEEE Trans. on Antennas and Propagation*, vol. AP-13, pp. 141–149, January 1965.
[2] H. Y. Yee, "Scattering of electromagnetic waves by circular dielectric-coated conducting cylinders with arbitrary cross sections," *IEEE Trans. on Antennas and Propagation (Communications)*, vol. AP-13, pp. 822–823, September 1965.
[3] H. Y. Yee and N. F. Audeh, "Uniform waveguides with arbitrary cross section considered by the point matching method," *IEEE Trans. on Microwave Theory and Techniques*, vol. MTT-13, pp. 847–851, November 1965.
[4] ——, "Attenuation constants of waveguides with general cross sections]" *IEEE Trans. on Microwave Theory and Techniques]* vol. MTT-14, pp. 252–253, May 1966.
[5] R. F. Harrinton, "On the calculation of scattering by conducting cylinders," *IEEE Trans. on Antennas and Propagation (Communications)*, vol. AP-13, pp. 812–813, September 1965.
[6] H. Y. Yee, "On determination of cutoff frequencies of waveguides with arbitrary cross section," *Proc. IEEE*, vol. 54, p. 64, January 1966.
[7] P. A. Laura, "Determination of cutoff frequencies of waveguides with arbitrary cross sections by point-matching," *Proc. IEEE (Correspondence)*, vol. 53, pp. 1660–1661, October 1965.
[8] ——, "Application of the point-matching method in waveguide problems," *IEEE Trans. on Microwave Theory and Techniques (Correspondence)*, vol. MTT-14, p. 251, May 1966.
[9] D. S. Jones, *The Theory of Electromagnetism*. New York: Macmillan, 1964, secs. 1.26, 1.34.
[10] G. N. Watson, *A Treatise on the Theory of Bessel Functions*, 2nd ed. Cambridge, England: Cambridge University Press, 1958, ch. 11.
[11] J. H. Richmond, "Digital computer solutions of the rigorous equations for scattering problems, *Proc. IEEE*, vol. 53, pp. 796–804, August 1965.
[12] P. C. Waterman, "Matrix formulation of scattering," *Proc. IEEE*, vol. 53, pp. 805–812, August 1965.
[13] H. Y. Yee and N. F. Audeh, "Cutoff frequencies of eccentric waveguides," *IEEE Trans. on Microwave Theory and Techniques*, vol. MTT-14, pp. 487–493, October 1966.

[2] Formerly with Sperry Rand Research Center, Sudbury, Mass.

Computer-Graphic Analysis of Dielectric Waveguides

The solutions to microwave problems are often enhanced by a visual representation of the fields, especially when the mathematical expressions are so complex as to resist physical interpretation by themselves. The particular graphical aid which is the subject of this correspondence is the field mapping, defined as a family of curves drawn parallel to the vector field being represented. Although such diagrams have been considered to be of great value since the early study of electrodynamics [1], the analytical and numerical complexities of modern engineering problems have inhibited their use on any wide scale. However, the current availability of digital computers, with compatible automatic plotting equipment, has made the numerical determination and display of field mappings a very practical adjunct to established analytical methods. The purpose of this correspondence is to illustrate the utility of field mapping by displaying the transverse electric field for the HE_{11} mode on a dielectric rod. It will be shown that the curvature of the field lines is in the opposite direction to that commonly assumed.

The equipment utilized in this study has been an IBM 7094 computer in conjunction with a Stromberg-Carlson 4020 microfilm unit. The computer performs all the calculations required to construct the field lines and stores the results on magnetic tape. These computed results are then used to control a cathode ray tube display, which is photographed and reproduced by standard methods.

Mathematically, electric field lines in a plane are the solution trajectories of the first-order differential equation

$$\frac{dy}{dx} = \tan\left[\alpha(x, y)\right] = \frac{E_y(x, y)}{E_x(x, y)} \qquad (1)$$

where α is the angle between the electric vector at (x, y) and the $+x$-axis. A first-order numerical approximation to that trajectory passing through a typical boundary point P_0 is depicted in Fig. 1. The calculation is made by using a first-order difference scheme, in which the point (x_{i+1}, y_{i+1}) is determined from (x_i, y_i) according to the relation

$$\begin{aligned} x_{i+1} &= x_i + \delta s \cos \alpha_i \\ y_{i+1} &= y_i + \delta s \sin \alpha_i \end{aligned} \qquad (2)$$

where δs is the path increment. Although this approximation can be refined to whatever accuracy is required [2], it is generally possible to find a path increment sufficiently small to give smooth and accurate contours without impractical amounts of computation.

The application to be considered in this correspondence is the determination of the transverse electric field for the fundamental (HE_{11}) mode of propagation along a dielectric rod with circular cross section. This mode is of significant interest in the analysis of dielectric waveguides [3], dielectric rod antennas [4] and more recently for its application to fiber optics and lasers [5]. Brown and Spector [6] and Snitzer [7] studied the field configuration when the slow wave phase velocity

Manuscript received July 28, 1966; revised September 21, 1966.

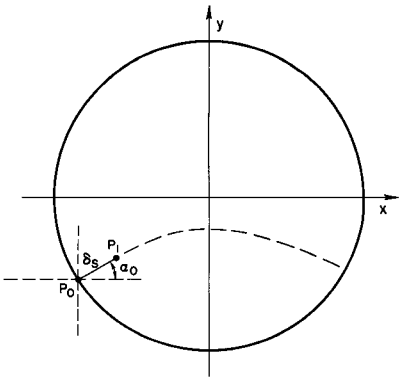

Fig. 1. First-order difference solution for the field lines.

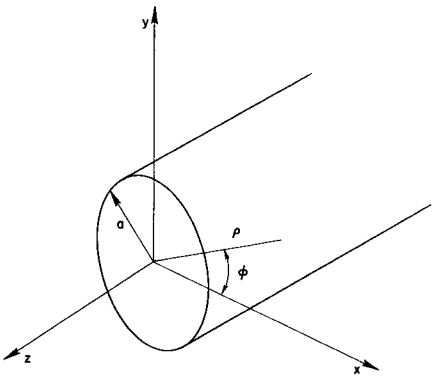

Fig. 2. Cylindrical geometry.

is near the free space velocity (assuming the rod to be in vacuum) and showed that in this limiting situation the field lines in the rod become straight and parallel. Although the more general case of arbitrary dielectric constant has never been accurately studied, it is commonly assumed that the field lines approach the configuration for the TE_{11} mode in a circular waveguide. The apparent justification for this conjecture is that as the wave is slowed down, the power becomes concentrated in the rod in the same way as power is contained within a metallic waveguide. Actually the situation is not analogous, since the fields do not vanish abruptly beyond the surface of a dielectric rod, with the result that there is always some power being transmitted in the region outside.

The cylindrical coordinate representation is shown in Fig. 2. The rod is assumed to have radius a, relative permittivity ϵ_r and a relative permeability of unity. As is well known, the electromagnetic field for the HE_{11} mode is derived from a linear combination of z-directed magnetic and electric Hertz vectors [3]. The electric field may be represented by

$$\boldsymbol{E} = \nabla \times (\boldsymbol{e}_z V_1) + \nabla \times (\boldsymbol{e}_z \times \nabla V_2) \qquad (3)$$

where, for the field inside

$$\begin{aligned} V_1^i &= AJ_1(\beta\rho)e^{ihz}\begin{cases}\cos\phi \\ \sin\phi\end{cases} \\ V_2^i &= BJ_1(\beta\rho)e^{ihz}\begin{cases}\sin\phi \\ \cos\phi\end{cases} \end{aligned} \qquad (4)$$

$$\beta^2 = \epsilon_r k_0^2 - h^2$$

$$k_0 = \text{free space wavenumber.} \qquad (5)$$